Sparse Parametric Imaging for direct parameter measurement: theory and phantom experiments

Ross A Little[1], Geoff J M Parker[1], and Chris Rose[1]
[1]*Centre for Imaging Sciences, University of Manchester, Manchester, United Kingdom*

Audience Members interested in morphological biomarker quantification in MRI, and post-Nyquist methods.

Purpose A large body of work in MRI involves measuring quantitative parameters, such as knee cartilage thickness[1] in osteoarthritis or hippocampal volume[2] in Alzheimer's disease. This is generally achieved through the acquisition of sufficient data to reconstruct one or more images from which measurements may be taken by manual or automated methods. Compressed sensing[3] has demonstrated that such images may be reconstructed from highly undersampled data. Here we introduce sparse parametric imaging (SPI), a novel method for quantifying morphological biomarkers directly, without the need to acquire sufficient data to fully reconstruct an image. We apply SPI to synthetic and physical phantoms, and show that it is possible to measure morphological quantities from simple geometrical shapes using just 1.6% of *k*-space.

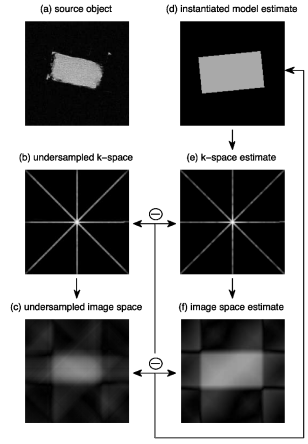

Figure 1: Illustration of SPI fitting method.

Theory Figure 1 illustrates the SPI method, in which (a) a source object is placed in the scanner, and (b) highly undersampled complex *k*-space measurements are acquired. Undersampled measurements may be Fourier transformed into (c) magnitude or complex undersampled image space. The source object is modelled by a function which maps from a low dimensional parameter $\boldsymbol{p}$ to image space; the function is constructed such that there is a mapping from $\boldsymbol{p}$ to the quantity of interest, *q*. An image instance (d) can be transformed to *k*-space, and from there to its undersampled *k*-space representation (e). This may be transformed into (f) the magnitude or complex undersampled image space. The quantity of interest *q* is estimated using an optimisation: $q = g(\arg\min_p f(\boldsymbol{p}, \boldsymbol{k}_u))$, where *g* is the mapping between the model parameter and the quantity of interest and *f* is an objective function that measures agreement between the image corresponding to $\boldsymbol{p}$ and undersampled *k*-space data $\boldsymbol{k}_u$. The function *f* can be stated in terms of $\boldsymbol{k}_u$, or alternatively in terms of undersampled complex or magnitude image space data.

Methods Two explicit models were applied to test the method. A disc model was parameterised by $\boldsymbol{d} = [r, x, y, s]$ where *r* denotes the radius, *x* and *y* denotes the origin and *s* denotes the signal intensity within the disc. The quantity of interest was the radius. A rectangle model was parameterised by $\boldsymbol{r} = [l_1, l_2, x, y, \theta, s]$ where additionally l_1 was the height, l_2 the width and θ the angle of rotation from the horizontal. The quantity of interest was the height. ***Synthetic phantoms:*** To characterise the potential of the method under ideal circumstances, 50 random synthetic disc and rectangle model instances were generated. These were transformed into *k*-space and undersampled using the pattern in Figure 1(b). Simulated annealing was used to minimise the objective function $\sum_n(|v[n]| - |v'[n]|)^2$, where $v[n]$ and $v'[n]$ describe respectively the n^{th} element of the acquired and estimated undersampled image space. ***Physical phantoms:*** Four physical phantoms were constructed from TX151 polysaccharide gel. One of these was formed within a cylindrical polymethyl methacrylate mould, and the remainder were formed within rectangular acrylonitrile butadiene styrene plastic moulds. The cylindrical phantom was scanned multiple times with a range of fields of view to simulate differently sized phantoms. Between each scan, the phantom was slightly shifted within the bore of the scanner before a complete complex image acquisition was made using a T_2-weighted turbo spin echo (TR 5000, TE 100, 192×192 matrix). For the three rectangular phantoms, fully sampled complex images were acquired using a T_1-weighted fast field echo (TR 15 ms, TE 5 ms, 192×192 matrix). The Fourier transform was applied to each image followed by retrospective undersampling of *k*-space using the pattern of figure 1(b) to simulate radial data acquisition. Ground truth measurements of disc radius and rectangle height were made (e.g., using OsiriX), and SPI was used to estimate the radius or height of the phantoms.

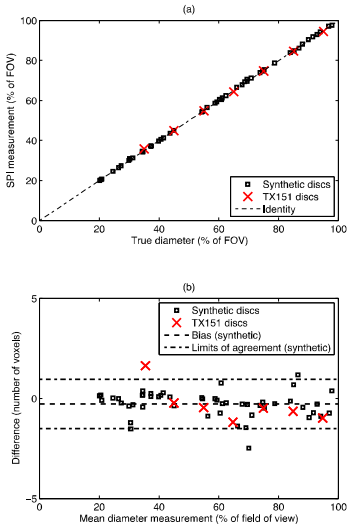

Figure 2(a) scatterplot of disc radius fits, (b) Bland-Altman plot of fits showing mean bias and limits of agreement.

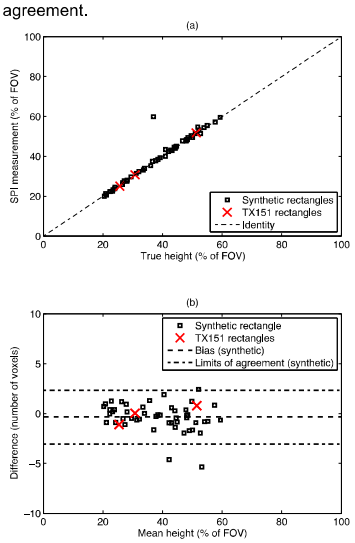

Figure 3(a) scatterplot of rectangle height fits, (b) Bland-Altman plot of fits showing mean bias and limits of agreement (excluding fit failure).

Results The measurements of the disc radius and rectangle height are shown in figures 2 and 3 respectively as (a) a scatterplot of the parameter of interest measurement and (b) a Bland-Altman plot with bias and limits of agreement. Bias and limits of agreement were calculated omitting one fit failure from the synthetic rectangle experiment. Each of the physical TX151 and synthetic circle radius measurements lie close to the line of identity (for both, $R^2 > 0.999$). The mean bias for the synthetic fits was less than one voxel with 95% limits of agreement of (-1.51, 0.96) voxels. For the rectangle heights, the TX151 physical phantom fits again had $R^2 > 0.999$. One of the synthetic test phantoms failed to fit and so the synthetic R^2 was 0.923. The mean bias for the synthetic rectangle fits (excluding the fit failure) was less than one voxel, with 95% limits of agreement of (-3.06, 2.35) voxels.

Discussion These results show the feasibility of SPI to directly measure parameters from highly undersampled *k*-space measurements without acquiring sufficient data to reconstruct a high fidelity image. While the objects and models used here are relatively simple, and there is a trivial mapping between the model parameters and the quantity of interest, we have demonstrated the feasibility of the approach. To use SPI to address more complex clinical problems, more sophisticated models and mappings must be used. While it may appear that anatomy is dramatically more complex, and may require very high dimensional models, approaches such as statistical appearance modelling[4] (SAM) demonstrate that realistic anatomical models may be built using, for example, 55 parameters[5], dramatically fewer than are required to reconstruct a 256x256 image, and substantially lower dimensionality than even a single line of *k*-space (e.g., 128 measurements). Such models may allow us to step directly from *k*-space data acquisition to accurate morphological or functional biomarker measurements, without explicit image reconstruction.

References 1. Williams et al., *Br J Radiol* 83(995):940–948, 2010. **2.** Schuff et al., *Brain* 132(Pt 4):1067-77, 2009. **3.** Lustig et al., *Magn Reson Med* 58:1182–1195, 2007. **4.** Cootes et al., *TMI PAMI* 23(6):681–685, 2001. **5.** Andreopoulos and Tsotsos, *Med Imag Anal* 12(3):335–357, 2008.